Positive thermopower of single bismuth nanowires

2004 J. Phys.: Condens. Matter 16 6507

(http://iopscience.iop.org/0953-8984/16/36/016)

INSTITUTE OF PHYSICS PUBLISHING JOURNAL OF PHYSICS: CONDENSED MATTER

J. Phys.: Condens. Matter **16** (2004) 6507–6518 PII: S0953-8984(04)83042-X

Positive thermopower of single bismuth nanowires

A D Grozav[1] **and E Condrea**

Laboratory of Semimetal Physics, Institute of Applied Physics, str. Academiei 5, Chisinau MD-2028, Republic of Moldova

E-mail: grozav@lises.asm.md

Received 24 June 2004
Published 27 August 2004
Online at stacks.iop.org/JPhysCM/16/6507
doi:10.1088/0953-8984/16/36/016

Abstract

The thermoelectric power and electrical resistance of pure bismuth nanowires have been measured in longitudinal magnetic fields up to $B = 20$ T at temperatures between 4.2 and 26 K. At $B = 0$, the 200 nm samples exhibit large values of thermopower (about +110 μV K^{-1} at 25 K), which are dominated by diffusion with no phonon drag being evident. Both the magnetoresistance and magnetothermopower show well-pronounced features generated by the diffuse surface scattering of hole carriers. In particular, the magnetothermopower offers the possibility of identifying the characteristic magnetic field, where the diameter of the hole Larmor orbit equals the wire diameter, as an extremum, in distinction from the magnetoresistance data, where the corresponding feature manifests as an inflection point. The frequencies of Shubnikov–de Haas oscillations were found to be consistent with the Fermi-surface parameters of bulk Bi. The contribution of holes to the charge transport in pure Bi nanowires is more significant than generally thought.

1. Introduction

Interest in the physical properties of bismuth nanowires has grown considerably in recent years, mainly due to their technological promise as very efficient thermoelectric elements in solid-state cooling devices. Theoretical calculations predict that Bi nanowires should have an enlarged thermoelectric figure-of-merit, which comes as a result of the enhancement in the thermoelectric power (TEP), S, due to an increase of the electronic density of states and the lowering of the thermal conductivity due to predominant phonon scattering at the boundaries [1]. To date, however, there is no reliable experimental evidence showing an improved thermoelectric efficiency in low-dimensional Bi structures.

Most previous experiments on micron and submicron Bi wires have been focused on measuring the electrical resistance, R, as a function of temperature, T, and magnetic

[1] Author to whom any correspondence should be addressed.

field, B [2–5]. By analogy with bulk Bi, the partial conductivity of holes was generally assumed to be small and, therefore, the classical size effects in the resistivity were unequivocally associated with the diffusive scattering of electrons at the wire boundaries. Comparatively little attention has been given to the study of the thermopower in Bi nanowires. To our knowledge, the first thermopower measurements on single glass-coated Bi wires were performed by Bodiul *et al* [6] at 80 K $\lesssim T \lesssim$ 300 K and $B = 0$. At $T \approx 80$ K, the TEP was found to be positive for wires with diameter $d \lesssim 800$ nm and negative for thicker samples. The change of the TEP sign was explained as being caused by a phonon drag mechanism in a wire with the size-induced quantized energy spectrum. The experimental results of [7] are similar and show that the nanowires with $d = 500, 300$ and 100 nm have increasing thermopower values of about +10, +30 and +40 μV K^{-1} at $T \approx 79$ K. By changing the band structure upon application of tensile strains, the TEP of these wires changes sign to negative and reaches values from -45 to about -85 μV K^{-1}. On the other hand, the TEP of 65 and 40 nm Bi/Al_2O_3 nanowire arrays is negative from room to liquid-helium temperatures with values between -20 and -25 μV K^{-1} at $T \approx 80$ K [8]. In a pure crystal of semimetal bismuth, the density of electrons N_e is naturally equal to the density of holes N_h. Analyses of the Shubnikov–de Haas (SdH) effect [9], however, have shown that the 200 nm Bi nanowires embedded in porous anodic alumina are distinctly n-type with $N_e/N_h \approx 3$ due to the presence of uncontrolled donor impurities. For these nanowires, the TEP was found to be positive below 30 K with a maximum of +5 μV K^{-1} around 10 K and negative above 30 K. Both the low-temperature TEP of Bi whiskers with $d \approx 1$ μm [10], which is of the order of a few μV K^{-1}, and the giant Seebeck effect observed in 9–15 nm Bi nanocomposites [11] have a strange feature: the sign of S varies from sample to sample. These facts would imply that besides classical and/or quantum size effects, other factors such as structural defects, impurity- and/or strain-induced alteration of the energy spectrum must also be considered for the understanding of various anomalies found in the transport properties of small diameter Bi wires.

In this work, we have studied the magnetic-field dependence of the thermopower and resistance of glass-coated Bi wires with $d = 200$ nm at temperatures below 26 K. These nanowires have anomalously large values of the thermopower ($\sim +100$ μV K^{-1}) and relatively high effective resistivities ($\rho \sim 100$ $\mu\Omega$ cm), but their frequencies of SdH oscillations remain those of bulk Bi. The TEP stays positive in longitudinal magnetic fields up to 20 T, where the surface scattering of charge carriers is negligible. Our analysis shows that the anomalous thermopower has a diffusion origin and is a consequence of the microstructure rather than the result of the strong scattering of electrons by the wire walls. The intensities of field at which the size-effect features appear on the magnetothermopower and magnetoresistance curves are essentially the same and correspond to a value at which the diameter of the hole cyclotron orbit equals d. The contribution of the phonon-drag effect was observed in a wire with $d = 1.1$ μm and $\rho < 10$ $\mu\Omega$ cm. The hole carriers play a more important role in determining the low-temperature transport properties of pure Bi nanowires than for their bulk counterparts.

2. Experimental results

Long Pyrex-coated Bi wires were fabricated using the same improved variant of the Taylor method as in [4–7]. This method, which is presently known as the glass-coated melt spinning method [12], consists in the melting of a metal in a glass tube by rf induction heating and drawing a glass capillary in which the molten metal is entrapped. We prepared two high-resistivity wire (HRW) samples with a nominal diameter of 200 ± 50 nm. The first sample (HRW-1) has a length between the ends of $L = 4.0$ mm and a residual resistance ratio RRR $= R(0, 300\ \text{K})/R(0, 4.2\ \text{K}) = 4.1$. For this sample, the measurements were

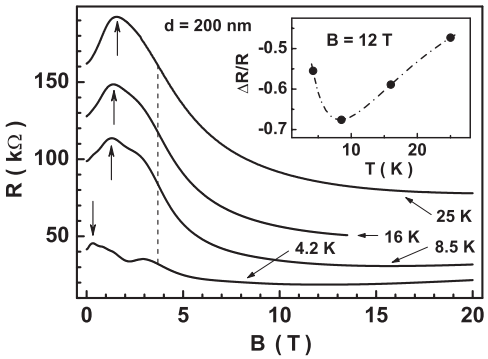

Figure 1. Resistance of the 200 nm nanowire sample HRW-1 as a function of longitudinal magnetic field at a fixed dc current of 0.1 μA and different temperatures. The vertical arrows denote the maxima points, and the vertical dashed line connects the inflection points. The inset shows the magnitude of the $\Delta R(B,T)/R(0,T)$ ratio for $B = 12$ T at various values of temperature.

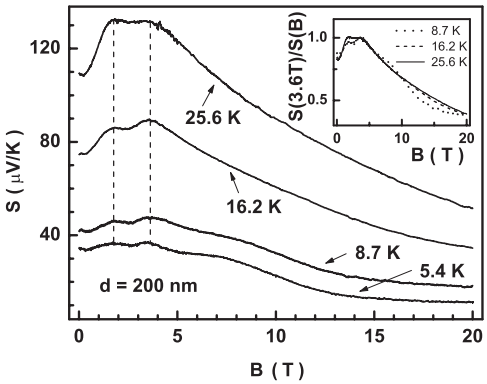

Figure 2. Thermopower of the 200 nm nanowire sample HRW-1 as a function of longitudinal magnetic field at various temperatures. The vertical dashed lines point to the thermopower maxima positions. The inset shows the B-dependence of the $S(3.6\ \mathrm{T},T)/S(B,T)$ ratio at $T = 8.7$, 16.2, and 25.6 K.

performed using a variable-temperature insert and a 20 T Bitter magnet at the High Magnetic Field Laboratory in Grenoble. For the second sample (HRW-2) with $L = 2.9$ mm and RRR $= 2.5$, the measurements were performed in the vicinity of liquid-helium temperature in a superconducting magnet up to 17 T at the NHMFL, Tallahassee. The cylindrical core of both samples has grown in a crystalline direction that makes an angle of about 19° with the C_1 axis in the bisector-trigonal plane C_1C_3 and so the binary axis C_2 is at right angles to the long wire axis. This orientation is the same as that observed in single Bi nanowires by Bodiul *et al* [6]. For comparison, we also studied a low-resistivity wire (LRW) sample with $d = 1.1$ μm, $L = 3.2$ mm and RRR ≈ 30. This RRR value is probably the largest among the Bi wires with $d \lesssim 2$ μm on which the transport measurements were ever performed and is comparable with the residual resistance ratios for some bulk Bi crystals, which were used for thermoelectric measurements [13]. For the LRW sample, the long axis was located in the C_1C_2 plane at an angle of about 12° with the C_1 axis [14]. The wire ends were wetted with liquid In–Ga eutectic and then accurately soldered with Wood's alloy to the two well-separated copper strips, which connect the sample to the current and voltage leads. Low dc currents ($0.1\ \mu\mathrm{A} \leqslant I \leqslant 1\ \mu\mathrm{A}$) were used to make sure that the voltage on the sample was a linear function of the applied current at any B. The thermopower was measured by a steady-state technique using a RuO_2 heater and two miniature RuO_2 thermometers. To have a reasonable signal-to-noise ratio, we were compelled to apply a relatively large temperature difference, $0.4\ \mathrm{K} \leqslant \Delta T \leqslant 0.8$ K. The magnetic-field-dependences of the TEP ($\boldsymbol{B} \parallel \boldsymbol{\nabla} T$) and electrical resistance ($\boldsymbol{B} \parallel \boldsymbol{I}$) were taken in separate runs within the same heating procedure.

The magnetoresistance and magnetothermopower data for sample HRW-1 are demonstrated in figures 1 and 2, respectively. Our MR results are qualitatively consistent with previous reports [3–5, 14–16]. At a certain field value, $B = B_\mathrm{m}$, the resistance reaches its maximum magnitude; in still higher fields R drops rapidly and then tends to saturation. As is shown in figure 1, the position of the resistance maximum shifts with temperature from $B_\mathrm{m} = 0.34$ T at 4.2 K to $B_\mathrm{m} = 1.56$ T at 25.4 K. The T-dependence of B_m is remarkably similar to that reported previously for Bi wires with $d = 3$–4 μm [14]. For the sample HRW-2, which has a

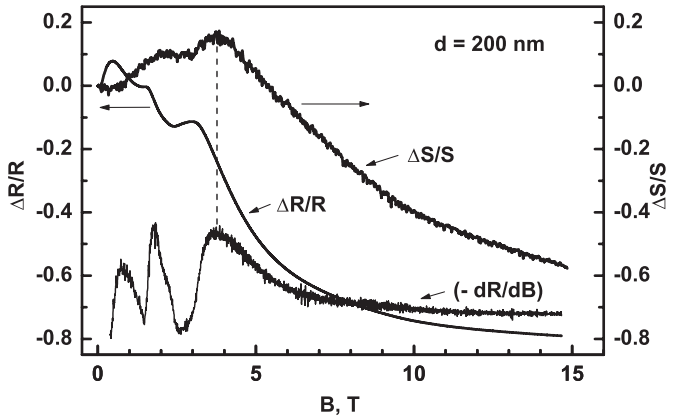

Figure 3. Longitudinal magnetoresistance and magnetothermopower of the 200 nm nanowire sample HRW-2 at $T = 4.2$ and 6.0 K, respectively, as a function of magnetic field. The bottom curve with an unspecified ordinate shows the negative derivative of the resistance with respect to B. The vertical dashed line indicates the magnetic field at which the cyclotron hole orbit equals the wire diameter.

lower value of RRR, $B_m(4.2\ \mathrm{K}) = 0.48$ T (figure 3). The emergence of the MR maximum can be associated with the manifestation of the classical size effect, when $l > d$, where l is the mean free path of charge carriers due to bulk scattering processes [17]. The decreasing resistance at $B > B_m$ is attributed to the suppression of the wire boundary scattering due to the focusing action of a longitudinal magnetic field. Consequently, the resistance in strong magnetic fields ($2r < d$, where r is the Larmor radius) is smaller than its zero-field value, giving rise to a negative magnetoresistance, $\Delta R(B,T)/R(0,T) = [R(B,T) - R(0,T)]/R(0,T) < 0$. Another important factor contributing to the appearance of negative longitudinal MR in Bi nanowires is the magnetic field dependence of the carrier density $N(B) \propto B$ [18]. This effect is of quantum nature and can be stronger than the classical one in fields where all electrons have fallen in the lowest level, i.e. the so-called the quantum limit state.

At $B > 0.5$ T, the $R(B)$ curves exhibited an oscillatory behaviour due to the Shubnikov-de Hass (SdH) effect. The SdH peaks are observed as the resistance maxima. As can be seen in figure 1, the largest SdH peak occurs around 3 T and is detected even at $T \approx 16$ K. However, it is very difficult to distinguish unambiguously the other SdH peaks against a rapid variation of the non-oscillatory part. Twofold differentiation of R with respect to B essentially eliminates disturbing background curvature and allows a detailed resolution in the quantum oscillations.

Figure 4 shows the second derivative $\partial^2 R/\partial B^2$ as a function of $1/B$ for the curve shown in figure 1 taken at $T = 4.2$ K. The frequency of oscillations, F, has been obtained from the slope of the peak number n against the reciprocal field $(1/B)$ at which the nth peak occurs. The straight line shown in figure 4 gives for the heavy electrons from two equivalent pockets B and C a frequency of $F_{BC} = 2.7 \pm 0.1$ T. Since the spin-splitting factor for these electrons is close to unity, their field of quantum limit B_{QBC} practically coincides with F_{BC}. Several hole peaks can be detected at $B > 4$ T (not visible in figure 1 because of the scale used), but they have deviations from periodicity in $1/B$ due to the field-induced increase in the Fermi energy [18]. For this reason, the quasi-classical frequency of hole oscillations F_h should be determined at fields below 4 T, where, however, the condition $2r < d$ is violated (see below) and, therefore, the possible quantum oscillations will also be non-periodic because of the truncated extreme hole orbits [16]. From the MR measurements on a thicker wire, $d \approx 650$ nm and RRR ≈ 12,

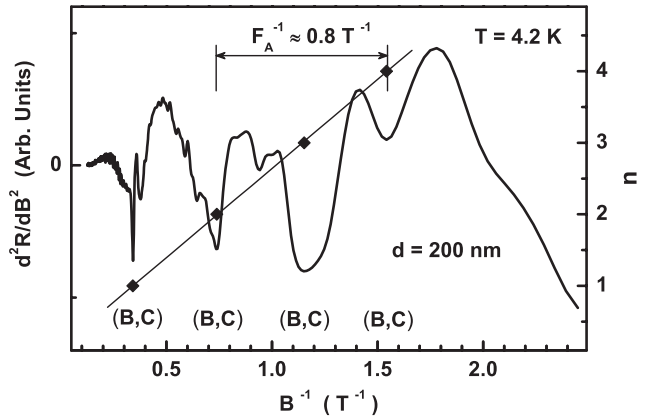

Figure 4. Second derivative of the resistance of the 200 nm nanowire sample HRW-1 at $T = 4.2$ K as a function of $1/B$. The straight line (right y-axis) is a fit to the plot of values of the peak number n versus the values of $1/B$ at the respective minima of $\partial^2 R/\partial B^2$ for the heavy (B, C)-electrons and indicates a frequency of 2.7 T.

with the same crystallographic orientation of the long axis, we obtained $F_{\rm h} \approx 16$ T and a value of the spin-splitting factor of about 1.7 for the range 1 T $\lesssim B \lesssim$ 3 T. The trace of the presence of light A-electrons with a frequency of $F_{\rm A} \approx 1.3$ T is related to some modulation of the amplitude of heavy-electron oscillations ($F_{\rm BC} \sim 2F_{\rm A}$) visible in figure 4. For sample HRW-2 (figure 3), we were able to resolve only one frequency: $F_{\rm BC} \approx 2.8$ T. Within the limits of experimental error, the frequencies and phases of the observed oscillations are in good agreement with the accepted values for bulk bismuth crystals: $F_{\rm A} = 1.26$ T; $F_{\rm BC} = 2.73$ T and $F_{\rm h} = 14.9$ T [18, 19]. Presumably, our 200 nm nanowires are too defective and/or thick to allow for a direct observation of quantum-size effects [1], which are predicted to decrease the frequencies of magnetic quantum oscillations.

On the other hand, it is natural to expect that the expansion of bismuth (3.32%) upon crystallization as well as the differences in thermoelastic properties of materials used in the fabrication of Bi/Pyrex composites will generate stresses at the interfaces and inside the wires. The presence of stresses should induce changes in the band-structure parameters, however, our results show that the influence of these stresses is negligible. This may be in the case when the Bi core and glass shell are not perfectly bonded and contracted separately with decreasing temperature or when a relief of these strains takes place. Nonetheless, as compared with quantum oscillations in the longitudinal magnetoresistance of good-quality bulk crystals [20], the SdH peaks are much broader with small relative amplitude at any field. Most probably, the significantly broadened Landau levels are due to the small-scale sample inhomogeneities created by stress relaxation.

As is shown in figure 1, both the zero- and high-field resistances have a monotonic metallic-like temperature dependence ($\partial R/\partial T > 0$). On the other hand, the high-field $\Delta R(B, T)/R(0, T)$ ratio reaches its maximal value (about -0.7 for $B > 10$ T) at a temperature above 4.2 K and close to $T^* = 8 \pm 1$ K, where a crossover from quadratic to quasilinear T-dependence of the zero-field resistance for micron Bi wires was observed previously [14]. The inset of figure 1 shows the non-monotonic T-dependence of the negative MR ratio for $B = 12$ T. An analysis of our previous MR data obtained on Bi wires with $d = 4.1$ and 3.6 μm at $2r \ll d$ [14] yields the same value for T^*. As yet we do not know if the observed extremum arises accidentally or due to physical origin. Simple estimations, however, show that the

position of this feature can be correlated with the condition $T_h^* = p_F^m s/k_B$ [21], where p_F^m is the maximum momentum of the hole Fermi surface, s is the sound velocity and k_B is Boltzmann's constant. Using $p_F^m = 4.9 \times 10^{-21}$ g cm s^{-1} [18] and $s = 2 \times 10^5$ cm s^{-1}($\mathbf{s} \parallel C_3$) [1, 21], we conclude that $T_h^* \approx 7$ K. The condition given above suggests that the temperature dependence of R should correlate with the change of the hole–phonon scattering probability as well as behaving linearly above 7 K. In our experiments between 8 and 25 K, the zero-field resistance increases almost linearly $R(0, T)/R(0, 300\ \text{K}) \propto \xi T$, where $\xi = 2.2 \times 10^{-2}$ and 1.6×10^{-2} K^{-1} for the 200 nm and 1.1 μm samples, respectively. It is surprising that the coefficient ξ is larger for the thinner wire with a smaller RRR. By comparing the resistivity data for 200 nm and 2 μm single Bi wires at $B = 0$ and $T < 50$ K, Gurvitch [2] observed a similar qualitative behaviour.

Figure 2 shows the magnetic field dependence of the TEP for the same sample whose resistance data are shown in figure 1. For 5 K $\lesssim T \lesssim$ 26 K, the TEP is positive at all magnetic fields. At low fields ($B \lesssim 0.5$ T), there are one or two weak peculiarities seen at different temperatures, but are poorly resolved owing to their small amplitude commensurate with the noise level in our experiments. At $B > 0.5$ T, the non-oscillatory part of the TEP increases with B, and then there is a relatively narrow range of fields (roughly 1.5 T $< B <$ 4 T) where it tends to saturate to a limiting value, particularly at $T \approx 25$ K. At this temperature, the magnitude of the 'saturated' TEP is about +135 μV K^{-1}. Closer examination of the S versus B curves reveals that the TEP passes through a local maximum at $B_{dS} = 1.7 \pm 0.1$ T, a minimum and reaches a maximum again at $B_{dS} = 3.6 \pm 0.1$ T. These two maxima yield a frequency of 3.7 T, which is absent in the MR data. An important feature in figures 2 and 3 is the strong drop in thermopower starting near the temperature-independent critical field B_{DS}, which is somewhat higher than B_{QBC}. This observation is elucidated in the inset of figure 2 by plotting $S(3.6\ \text{T}, T)/S(B, T)$ versus B at three temperatures. At $B > B_{DS}$, where the quantum limit for all the electrons has already been reached, the holes are still in the quasi-classical range of magnetic fields, and one can observe weak oscillations of S resulting from the quantization of their spectrum. At $T \approx 16$ K and above, the thermal smearing makes these high-field hole oscillations unobservable, unlike the above-mentioned two maxima located at lower fields, which have a distinct amplitude even at $T \approx 25$ K. As shown in the inset of figure 2, the high-field non-oscillatory part of $S(B_{DS}, T)/S(B, T)$ is almost independent of T, and this may mean that the observed decrease in S above B_{DS} is strongly affected by the magnetic field dependence of the density of states [18]. Note that at fields higher than 8 T, the non-oscillatory TEP decreases almost exponentially with B and, in contrast to the MR, does not show saturation up to 20 T.

When the TEP is plotted versus temperature (figure 5(a)), the corresponding data show a quasi-linear behaviour with a positive slope ($\partial S/\partial T > 0$) both in the low ($2r > d$) and high ($2r < d$) field regimes:

$$S = \alpha + \beta T, \tag{1}$$

where $\beta \approx$ +3.8, +4.8, and +2.0 μV K^{-2} at $B = 0, 3.6$ and 20 T, respectively, while the parameter α changes from about +10 μV K^{-1} at $B = 0$ T to about zero at $B = 20$ T. It is interesting to note that β varies non-monotonically with B. Taking into account the uncertainty in the fitting procedure (± 0.2 μV K^{-2}) as well as the accuracy of the thermopower measurements, the values of α cannot be considered as conclusive.

For comparison, we report in figure 5(b) the TEP values at $B = 0$ and 15 T for the 1.1 μm Bi wire. For this sample, the zero-field TEP decreases from about +45 μV K^{-1} at 6.6 K to about +19 μV K^{-1} at 25.4 K. At high magnetic fields, the TEP also stays positive. The T dependence of S is non-linear with a negative slope ($\partial S/\partial T < 0$) at $B = 0$, i.e. is qualitatively similar

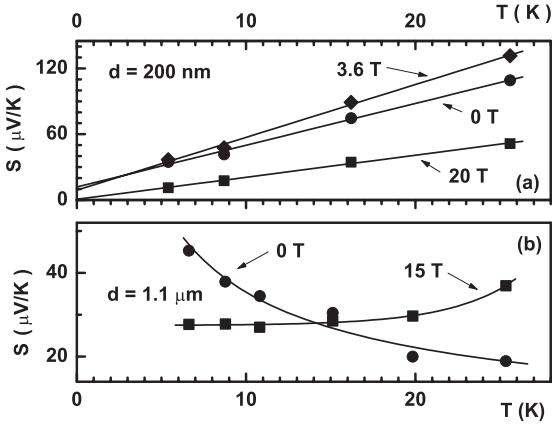

Figure 5. Change in the thermopower with temperature at various values of longitudinal magnetic field for the 200 nm nanowire sample HRW-1 (a) and 1.1 μm wire sample LRW (b).

to that found for bulk Bi crystals in the same temperature range, where the magnitude of the phonon-drag thermopower S_g exceeds or is comparable to the diffusion thermopower S_d [22].

3. Discussion

The most surprising aspect of our measurements is the fact that the TEP of the 200 nm Bi nanowires can be very large at relatively low temperatures. For example, $S(0, 25\ \mathrm{K}) \approx +110\ \mu\mathrm{V\ K^{-1}}$, which exceeds the thermopower (negative) of bulk Bi by a factor of $\sim$7 for $\boldsymbol{\nabla} T \perp C_3$ and by a factor of $\sim$3 for $\boldsymbol{\nabla} T \parallel C_3$ at the same temperature [23]. Considering the quasi-linear $S(B, T) \propto T$ dependence of the type, indicated by straight lines in figure 5(a) and fitted by equation (1), we may tentatively associate the observed TEP with a diffusion transport mechanism.

Standard explanations of the diffusion thermoelectric power rely on the Mott expression [24]

$$S_d = \pi^2 k_B^2 T(\partial \ln \sigma / \partial E)/3e = \beta T, \tag{2}$$

where e is the charge of the carriers, σ is the electrical conductivity, and E is the carrier energy. Theoretical calculations show than an enhancement in the density of states due to the quantum size effect may generate large contributions to the thermopower of bismuth through the term $(\partial \ln \sigma / \partial E)$ [1]. For our samples, however, no dependence of the SdH frequencies on wire diameter is observed and, therefore, the size quantization of the electron energy spectrum does not appear to represent a significant effect.

In a two band model of a semimetal with $N_e = N_h$, the thermopower may be written rather generally as

$$S_d = (\nu S_{de} + S_{dh})/(\nu + 1), \tag{3}$$

where $\nu = \mu_e/\mu_h$; μ_e and μ_h are the mobilities of the electrons and holes, respectively, and $S_{de} = \beta_e T$ and $S_{dh} = \beta_h T$ are the partial thermopowers of the electrons and holes, respectively. At temperatures below 50–70 K, the zero-field TEP of bulk Bi single-crystals does indeed show a standard diffusion behaviour $S_d = \beta T$ with $\beta \approx -0.66\ \mu\mathrm{V\ K^{-2}}$ for $\boldsymbol{\nabla} T \parallel C_1$ [25]. In pure Bi, $|S_{dh}/S_{de}| \sim$ 2–2.5 and the negative sign of β may arise only from the difference in electron and hole mobilities. Since the diffusion TEP cannot exceed a few $\mu\mathrm{V\ K^{-1}}$ at liquid-helium temperatures, the large values of positive TEP ($\lesssim +70\mu\mathrm{V\ K^{-1}}$),

which were observed experimentally in bulk Bi between 2 and 4 K, are considered to be a direct manifestation of the phonon drag effect [22].

The thermopower of our Bi/Pyrex nanowires, however, has large positive values at temperatures about one order of magnitude higher and, as mentioned in the introduction, the positive sign of $S(0, T)$ persists up to liquid-nitrogen temperatures, where the manifestation of the phonon drag effect in semimetals is unlikely. According to equation (3), the large positive values of $S_d \sim S_{dh}$ can be expected only if $\nu \ll 1$. For an isotropic parabolic spectrum and an energy-independent relaxation time, the logarithmic derivative in equation (1) is simply $(2E_F/3)^{-1}$, leading to the expression [24]

$$S_d = \pi^2 k_B^2 T/2eE_F. \tag{4}$$

Using this equation and the Fermi energy for hole carriers, $E_F \approx 11$ meV for $B = 0$ [25], we can roughly estimate the quantity $\beta_h = S_d/T \approx +3.3\,\mu\text{V K}^{-2}$. This value is surprisingly close to the slope of the zero-field data shown in figure 5(a), suggesting that the electron component of the total TEP is very small in our 200 nm Bi nanowires. We consider the measured slope of $S(0, T)$ as being close to the upper bound for the positive diffusion TEP in pure nanowires having the same band structure parameters as those in bulk bismuth. The value of β for a particular sample will depend on ν. However, the physical reason for the different changes in the electron and hole mobilities under the influence of wire diameter and/or quality is not obvious.

At the same time, the above formulae for the diffusion contribution cannot be applied to the 1.1 μm wire sample, which has a non-linear temperature dependence of the thermopower with $\partial S/\partial T < 0$ at $B = 0$ (figure 5(b)). In standard low-temperature measurements of bulk Bi crystals [22] such behaviour is associated with the phonon drag effect whereby the phonon flux from the hot end of the sample to the cold end drags additional charge carriers to the cold end of the sample. To a first approximation, the data can be described by assuming

$$S = S_d + S_g = \beta T + \gamma/T, \tag{5}$$

where $S_g = \gamma/T$ is the phonon drag term, which is valid only for the high-temperature side of the so-called 'phonon drag' peak, where anharmonic scattering limits the phonon lifetime [24]. Over the range 5–25 K, the fit yields $\gamma \approx +270\ \mu$V and $\beta \approx +0.9\ \mu\text{V K}^{-2}$. Thus even for the low-resistivity wire the linear diffusion term coefficient β is positive, though it has a significantly smaller magnitude than that obtained for the 200 nm wire. Generally speaking, these wires have different crystalline orientations along the sample length and a direct comparison between their transport properties cannot be made. However, the trend observed for the S_d values is reasonable when compared to the TEP data obtained on submicron Bi nanowires near liquid-nitrogen temperature [6]. According to equation (3), the decrease of β might be attributed to an increase in the ratio of electrons to hole mobility, which in turn can be accounted for by either an increase in wire diameter (due to a diminished influence of the surface scattering of electrons) or a decrease in the concentration of structural imperfections; a more definite conclusion requires an analysis of the galvanomagnetic data (see below). As shown in figure 5(b), the S versus T curves have different shapes at $B = 0$ and 15 T. The observed change from $\partial S/\partial T < 0$ to $\partial S/\partial T > 0$ suggests that increasing the magnetic field enhances the relative contribution of the diffusion TEP and decreases the phonon drag contribution.

Some parameters for the 200 nm wire samples can be estimated using the size-effect features of resistance in the longitudinal magnetic field and the energy-spectrum parameters of bulk Bi. It has been shown in [14] that the magnetoresistance curves contain a maximum at

$$B_m \approx cp_F/e(dl)^{1/2} \tag{6}$$

and an inflection point at

$$B_{DR} \approx 2cp_F/ed, \tag{7}$$

which allows us to extract information on the Fermi momentum p_F in the plane perpendicular to $\boldsymbol{B}$ and the bulk mean free path of the charge carrier group l that undergoes the most intensive incoherent (diffusive) surface scattering in Bi wires with $d \lesssim l$. The major advantages of measurements using Bi wires with micron diameters, compared with measurements made on nanowires, are that the size-induced feature appears in quasiclassical magnetic fields ($B < B_{QBC}$) [5, 14], when the interpretation of the experimental data is not complicated by the field-induced changes of the energy-spectrum parameters [18], and smaller relative errors in the determination of the current-carrying core diameter of composite samples are made [2]. The dependence of B_m on l in equation (6) agrees well with the theory of the galvanomagnetic size effect for thin films [17], while the conclusion that the hole carriers dominate the electrical conductivity in micron Bi wires [14] was confirmed independently for the present nanowire samples by the thermopower measurements. For both 200 nm wires, the MR curves display an inflection point (a minimum on $\partial R/\partial B$) at $B_{DR} = 3.7 \pm 0.1$ T (figures 1 and 3). This feature is well-resolved even at $T \approx 25$ K, where the SdH oscillations disappear. Since the Fermi-surface parameters for bulk Bi are known with a high degree of accuracy, we can use formula (7) for an estimation of the effective wire diameter. For the holes in our experimental configuration, $p_F \approx 4.5 \times 10^{-21}$ g cm s^{-1} [18], and, consequently, $d \approx 150$ nm, in fairly good agreement with the 200 ± 50 nm derived from $R(0, 300\ \text{K}) = (4L/\pi d^2)\rho(0, 300\ \text{K})$, where $\rho(0, 300\ \text{K}) = 120$–$200\ \mu\Omega$ cm [2]. Substituting the values for p_F, d and B_m in equation (6) yields $l_h(4.2\ \text{K}) \approx 3.4$ and 2.3 μm for samples HRW-1 and HRW-2, respectively. These values of hole mean free path are about two orders of magnitude smaller than those in high-quality bulk crystals [26]. For Bi wires with $d = 1$–$4\ \mu$m and RRR = 20–30, having $B_m = 0.04$–0.1 T and different crystalline orientations [5, 14], we estimate $l_h(4.2\ \text{K}) \sim 10$–$20\ \mu$m.

It should also be stated that for 200 nm nanowires, the condition $2r \approx d$ is satisfied in fields somewhat higher than B_Q, where the volume of the hole pocket begins to increase in size. Assuming that $p_F(B_{DR}) = p_F[N_h(B_{DR})/N_h]^{1/3}$ and by using $N_h(B_{DR})/N_h \approx 1.3$ for $\boldsymbol{B} \parallel C_1$ [18], one finds $p_F(B_{DR}) \approx 4.9 \times 10^{-21}$ g cm s^{-1}, which leads to $d \approx 170$ nm according to equation (5). Thus, the field-induced error in the above estimation of d is 10–15%, however, in the case of thinner nanowires it may be much more important to take into account the B dependence of p_F.

As can be seen from figures 2 and 3, the increase in the value of the positive TEP takes place in the field region, where the condition $(l_h d)^{1/2} > r > d/2$ is satisfied, and, therefore, may be a reflection of the classical size effect in a longitudinal magnetic field, when the suppression of the boundary scattering would be stronger for holes than for electrons. The bottom curve in figure 3 shows that the negative derivative of the resistance with respect to the magnetic field resembles (but does not coincide with) the behaviour of S-versus-B curve, in accordance with the more general expression for the diffusion thermopower (equation (2)). Unlike the first peak (near 0.8 T at 4.2 K) on this derivative, the positions of the other two maxima at $B \approx 1.8$ and 3.7 T show no temperature dependence up to $T \approx 25$ K. Since $B_{DS} \approx B_{DR}$, we can conclude that the high-field TEP peak reflects the transition from $2r > d$ to $2r < d$. Thus, the B-dependence of the diffusion TEP offers the possibility of identifying the characteristic field, where $2r \approx d$, as an extremum, in distinction from the magnetoresistance data, where this feature manifests as an inflection point. This type of size-induced feature can be observed only if the reflection of holes at the wire walls is not totally specular. To the best of our knowledge, this is the first observation of the size effects in the magnetothermopower of Bi nanowires.

Since $B_{DS}/B_{ds} \approx 2$, the low-field TEP hump can be regarded as another size-induced feature, where $r \approx d$. However, the status of this 'characteristic feature' is somewhat uncertain [16], and additional experiments are needed to obtain conclusive evidence that the magnetotransport properties of Bi nanowires undergo substantial changes at $r \approx d$. For the light and heavy electrons, the condition $2r \approx 150$–200 nm is satisfied at fields 0.5–0.7 T ($p_F = 0.8 \times 10^{-21}$ g cm s^{-1}) and 0.7–0.9 T ($p_F = 1.1 \times 10^{-21}$ g cm s^{-1}), respectively. At these values of field, however, the amplitude of supposed electron-generated features (figure 2) is practically indistinguishable from the measurement noise. It follows thence that, in distinction from the holes, the electrons should exhibit nearly specular scattering from a Bi/Pyrex interface and, therefore, do not contribute essentially to classical size effects in the thermopower and electric resistivity. This also implies that the apparent small conductivity of electrons is a consequence of bulk structural disorder rather than the result of rough surfaces. A significant influence of the ordinary diffuse reflection [27] may be expected in the case when the linear dimensions of the surface roughness or shell-induced damages are of the order of the Fermi wavelength $\lambda_F \propto (p_F)^{-1}$, which is about 10 nm for holes and a few tens of nanometres for electrons. We should stress the point that the specular scattering is an important condition for the quantum-size effect to manifest, a regime where the electronic transport in nearly perfect Bi nanowires is well theoretically understood [1]. In this regime, the Fermi wavelength increases with decreasing d and, therefore, even the influence of diffuse surface scattering of holes on the magnetotransport properties of quantum Bi nanowires may be suppressed appreciably.

A very strong specular scattering of electrons also follows from the experiments of Tsoi and co-workers [28, 29] on bulk single-crystals of Bi and Sb. Using a technique based on the focusing of the charge carriers by a transverse magnetic field, these authors obtained the direct observation of a large difference between the probabilities of specular reflection for electrons, $W_e \approx 0.8$, and holes, $W_h \approx 0.2$, falling at normal incidence to the free surface (for a Bi/silica interface, $W_e \approx 0.90$–0.95). In our experiments, a similar difference between W_e and W_h explains the absence of well-defined size-effect features corresponding to electrons, but does not explain the positive sign of the diffusion TEP, which we consider to be an explicit demonstration of the unusual scattering properties of the conduction charges in glass-coated Bi nanowires. At this stage we can only speculate on the nature of the physical mechanism that might plausibly produce the inequality $\mu_h \gg \mu_e$ under such conditions that $W_h < 1$ and $W_e \to 1$.

In compensated semimetals, any type of surface or bulk defects that scatter electrons more effectively than holes is likely to enhance the positive contribution to the total S (equation (3)). Since the TEP remains hole-like in strong magnetic fields, where all the electrons moves quasi-one-dimensionally parallel to the wire axis, the surface scattering is probably not a mechanism determinative of the S sign. The suppression of the electron contribution seems to be related to the complexity of the wire microstructure. A possible mechanism responsible for the enhanced values of the positive TEP and resistivity may be based on the model of selective carrier scattering by potential barriers [30]. Such barriers usually arise at grain boundaries, where some changes in the potential occur due to the enhanced degree of disorder (dangling bonds, local stresses, etc). In this context, our Bi nanowires can be regarded as consisting of a number of elongated crystallites separated by 'transverse' boundaries, which act as energy barriers with charge-selective properties: the electrons are scattered much stronger than holes. Note that the hole character of the charge carriers was also seen in bulk Bi crystals after plastic deformation [31] and in mosaic Bi films with thicknesses varying between 130 and 300 nm [32]. After heat-treatment procedures, these films become 'homogeneous', a medium of well-connected micron-size grains, which exhibit the positive Hall coefficient and detectable SdH oscillations.

It is interesting to note that to explain the dramatic difference between W_e and W_h for a free surface of bulk Sb crystal, Tsoi and co-workers [28, 29] used the concept of 'electron-reflecting hole-transmitting' potential barriers originating from surface states and band bending effects. Since $W_e > W_h$, the donor-type surface states (negatively charged) are considered to be responsible for the band bending, which creates a barrier reflecting electrons and, at the same time, provides conditions favourable for holes to be scattered by the surface roughness. In order to interpret our experiments, one has to assume that the potential barriers with the similar charge-selective scattering properties are present not only at the Bi/Pyrex interface, where they suppress almost completely the diffuse surface scattering of electron carriers, but also near the crystallite boundaries within the nanowire, where they cause backscattering of electrons, producing a large contribution to the residual resistivity. Note that the presence of internal electron-reflecting hole-transmitting barriers may lead to a localization-like behaviour for the electrons and a metallic behaviour for the holes. A similar scenario in the sense of localized electrons and delocalized holes has been invoked by Azbel [33] to interpret the metallic conductivity observed in the experiments on high-resistivity Bi and Bi–6 at.% Sb whiskers with $d = 140$–210 nm from $T = 20$ K down to 0.4 K [34]. The influence of potential disorder induced by crystallite boundaries may also provide an explanation to the observed substantial quantitative and qualitative differences in thermopower measurements in different wire samples (figure 5), since any change in sample preparation and heat-treatment history can give rise to totally different crystallite-boundary structures and properties.

Finally, the above information allows us to conclude that the SdH oscillations in Bi nanowires originate from the crystallites with bulk-like carrier densities, while the large values of the thermopower and resistivity are determined by the boundaries between crystallites, which reduce the mobility of electrons to such an extent that the majority of the conductivity comes from holes. The strong scattering of electrons by internal boundaries is superimposed on the smaller classical size effect produced by the diffuse scattering of holes at the wire walls.

4. Summary

We have demonstrated that the hole carriers dominate the charge transport in pure Bi nanowires at temperatures below 26 K. The diffuse boundary scattering of holes generates various types of size-effect features both in the longitudinal magnetoresistance and diffusion magnetothermopower. At 4.2 K, the hole mean free path was found to be larger than the wire diameter, but about two orders of magnitude less than that in the high-quality single crystals. This result is consistent with the diffusion origin of the TEP and the small amplitude of SdH oscillations in high-resistivity 200 nm samples. The absence of well-defined size-effect features corresponding to electrons indicates that the reflections of the majority of these carriers at wire boundary are specular. The large positive TEP values are attributed to the presence of bulk structural defects, which strongly diminish the electron contribution without affecting the band structure inside the nanowire crystallites. We have observed the phonon-drag effect ($S \propto 1/T$) in the 1.1 μm wire that has a higher crystalline perfection as compared with the 200 nm samples. More work is needed to elucidate the precise nature of the defects responsible for the enhancement of TEP at low temperatures as well as to establish if the structural imperfections may be exploited to improve the efficiency of thermoelectric nanowires.

Acknowledgments

One of the authors (EC) acknowledges support from the High Magnetic Field Laboratory in Grenoble and would also like to thank Dr A G M Jansen and Dr I Sheikin for valuable

assistance in conducting experiments. A portion of this work was performed at the National High Magnetic Field Laboratory (Tallahassee), which was supported by the NIS Visitors Program, and the authors are particularly appreciative of the help provided at that facility by Dr B Brandt. The authors are pleased to acknowledge the support for this work by the MRDA/CRDF Award No MP2-3046.

References

[1] Lin Y-M, Sun X and Dresselhaus M S 2000 *Phys. Rev.* B **62** 4610
[2] Gurvitch M J 1980 *J. Low. Temp. Phys.* **38** 777
[3] Zhang Z, Sun X, Dresselhaus M S, Ying J Y and Heremans J 2000 *Phys. Rev.* B **61** 4850
[4] Brandt N B, Gitsu D V, Dolma V A and Ponomarev Ya A 1987 *Zh. Eksp. Teor. Fiz.* **92** 913
Brandt N B, Gitsu D V, Dolma V A and Ponomarev Ya A 1987 *Sov. Phys.—JETP* **65** 515 (Engl. Transl.)
[5] Gitsu D V, Grozav A D, Konopko L A and Munteanu F M 1983 *Fiz. Tverd. Tela* **25** 2960
Gitsu D V, Grozav A D, Konopko L A and Munteanu F M 1983 *Sov. Phys.—Sold State* **25** 1707 (Engl. Transl.)
[6] Bodiul P P, Gitsu D V, Dolma V A, Miglei M F and Zegrea G G 1979 *Phys. Status Solidi* a **53** 87
[7] Condrea E, Grozav A D and Leporda N I 2001 *Proc. 6th European Workshop on Thermoelectrics of the European Thermoelectric Society (Freiburg, Germany, Sept. 2001)* (Freiburg: Fraunhofer Institute of Physical Measurement Techniques IPM)
[8] Lin Y-M, Rabin O, Cronin S B, Ying J Y and Dresselhaus M S 2002 *Appl. Phys. Lett.* **81** 2403
[9] Heremans J and Trush C M 1999 *Phys. Rev.* B **59** 12579
[10] Gaidukov Yu P, Danilova N P and Nikiforenko E V 1984 *Pis. Zh. Eksp. Teor. Fiz.* **39** 522
[11] Heremans J P, Thrush C M, Morelli D T and Wu M-C 2002 *Phys. Rev. Lett.* **88** 216801
[12] Hagiwara M and Inoue A 1993 *Production Techniques of Alloy Wires by Rapid Solidification in Rapidly Solidified Alloys* ed H H Liebermann (New York: Dekker) p 141
[13] Uher C and Pratt W P Jr 1978 *J. Phys. F: Met. Phys.* **8** 1979
[14] Grozav A D and Leporda N I 1996 *Fiz. Tverd. Tela* **38** 1924
Grozav A D and Leporda N I 1996 *Phys. Solid State* **38** 1063 (Engl. Transl.)
[15] Grozav A D and Leporda N I 1996 *Czech. J. Phys.* **46** (Suppl. S4) 2353
[16] Gaidukov Yu P 1984 *Usp. Fiz. Nauk* **142** 571
Gaidukov Yu P 1984 *Sov. Phys.—Usp.* **27** 256 (Engl. Transl.)
[17] Kao Y H 1965 *Phys. Rev.* **138** A1412
[18] Edel'man V S 1977 *Usp. Fiz. Nauk* **123** 257
Edel'man V S 1977 *Sov. Phys.—Usp.* **20** 819 (Engl. Transl.)
[19] Brown R D III 1970 *Phys. Rev.* B **2** 928
[20] Tanuma S and Inada R 1975 *Phys. Condens. Matter* **19** 95
[21] Gollnest H J, Kuka G, Broune W and Herrmann R 1979 *Phys. Status Solidi* b **91** 177
[22] Issi J-P 1979 *Aust. J. Phys.* **32** 585
[23] Farag B S and Tanuma S 1976 *Technical Report of ISSP (Series B, No. 18)* (Tokyo: Institute for Solid State Physics. University of Tokyo) pp 1–138
[24] Blatt F J, Schroeder P A, Foiles C L and Greig D 1976 *Thermoelectric Power of Metals* (New York: Plenum)
[25] Heremans J and Hansen O P 1979 *J. Phys. C: Solid State Phys.* **12** 3483
[26] Hartmann R 1969 *Phys. Rev.* **181** 1070
[27] Zhilyaev I N and Kopylov V N 1980 *Fiz. Nizk. Temp.* **6** 1344
[28] Falkovsky L A 1983 *Adv. Phys.* **32** 753
[29] Tsoi V S and Razgonov I I 1976 *Pis. Zh. Eksp. Teor. Fiz.* **23** 107
Sveklo I F and Tsoi V S 1992 *Pis. Zh. Eksp. Teor. Fiz.* **56** 536
[30] Ravich Y I 1995 *CRC Handbook of Thermoelectrics* ed D M Rowe (New York: CRC Press) chapter 7, pp 67–73
[31] Bogod Ya A and Krasovitski Vit B 1978 *Fiz. Nizk. Temp.* **4** 996
[32] Komnik Yu F, Andrievskii V V and Butenko A V 1981 *Fiz. Nizk. Temp.* **7** 1127
[33] Azbel M Ya 1983 *Phys. Rev.* B **27** 3852
[34] Overcash D R, Ratnam B A, Skove M J and Stillwell E P 1980 *Phys. Rev. Lett.* **44** 1348